

K. SZTWIERTNIA*, J. KAWAŁKO*, M. BIEDA*, K. BERENT*

MICROSTRUCTURE OF POLYCRYSTALLINE ZINC SUBJECTED TO PLASTIC DEFORMATION BY COMPLEX LOADING

MIKROSTRUKTURA POLIKRYSTALICZNEGO CYNKU ODKSZTAŁCZONEGO PLASTYCZNIE W ZŁOŻONYM SCHEMACIE DEFORMACJI

Polycrystalline, high purity (99,995%) zinc ingot was subjected to KoBo type extrusion in room temperature. Material was extruded to form of a 2 mm diameter wire, extrusion die oscillated during process by an angle $\pm 8^\circ$ at a frequency of 5 Hz and the extrusion speed was 0.5 mm/s. Final product was tested for tensile strength and yielded $R_{0,2} \approx 150\text{MPa}$ and $R_m \approx 250\text{MPa}$. Microstructure of both extruded and initial materials was investigated by means of high resolution Electron Backscatter Diffraction (EBSD) in Quanta 3D FEG scanning electron microscope (SEM). Observations revealed that microstructure of extruded zinc sample is highly heterogeneous and consists of grains elongated slightly in the direction of extrusion. Grains dimensions ranges from over one hundred microns down to submicron scale while grains in the non-deformed material are equiaxed with mean diameter of approximately 200 microns. Other microstructure features such as intergranular bands and partly fragmented primary grains with subgrain structure are observed. Furthermore detailed study of local microstrains by Image Quality Factor analysis are performed. Presence of Geometrically Necessary and Statistically Stored Dislocations is assessed. Thick areas of highly distorted lattice adjacent to High Angle Grain Boundaries are revealed. Microstrain mapping suggest composite-like microstructure of deformed material, that might explain its superior mechanical properties.

Keywords: Zinc, Plastic deformation, EBSD, KoBo, Strain mapping

Polikrystaliczny cynk o wysokiej czystości (99,995%) został poddany wyciskaniu metodą KoBo w temperaturze pokojowej. Materiał został wyciśnięty do postaci drutu o średnicy 2 mm. Matryca podczas procesu odkształcania oscylowała o kąt $\pm 8^\circ$ z częstotliwością 5 Hz a prędkość wyciskania ustalono na 0.5 mm/s. Produkt końcowy poddany został testowi wytrzymałości na rozciąganie, uzyskane wyniki to $R_{0,2} \approx 150\text{MPa}$ and $R_m \approx 250\text{MPa}$. Mikrostruktura materiału wyjściowego i odkształconego została zbadana metodami wysoko rozdzielczej dyfrakcji elektronów wstecznie rozproszonych (EBSD) w skaningowym mikroskopie elektronowym Quanta 3D FEG (SEM). Przeprowadzone obserwacje wskazują na silnie heterogeniczny charakter mikrostruktury odkształconego cynku, która składa się z ziarn lekko wydłużonych w kierunku wyciskania. Rozmiary ziarn wahają się od ponad stu mikrometrów do poniżej jednego mikrometra, podczas gdy materiał nieodkształcony składa się z równoosiowych ziarn o średnich rozmiarach rzędu 200 mikrometrów. Inne zaobserwowane cechy mikrostruktury to ciągnące się przez całą próbkę pasma drobnych ziarn oraz częściowo rozdrobnione ziarna pierwotne ze strukturą podziarnową. Ponadto wykorzystując rozkłady parametru jakości obrazu dyfrakcyjnego przeprowadzono szczegółową analizę pól mikroodkształceń. Dokonano oceny obecności dyslokacji geometrycznie niezbędnych oraz nagromadzeń dyslokacji przypadkowych. Zidentyfikowano szerokie obszary silnie zniekształconej sieci krystalicznej rozciągnięte wzdłuż granic dużego kąta. Analiza rozkładu mikroodkształceń w materiale odkształconym wskazuje na podobieństwo mikrostruktury tego materiału do struktury kompozytu. Taka charakterystyka może tłumaczyć znaczny wzrost właściwości mechanicznych materiału po wyciskaniu KoBo.

1. Introduction

Severe Plastic Deformation methods have gained significant interest in past years, mainly due to possibility of fabrication nano- and ultrafine-crystalline materials [1,2] with considerably increased mechanical strength, according to Hall – Petch relation[3,4].

KoBo type extrusion [5] is a method of plastic forming that doesn't relate completely to classic SPD definition, it is however also capable of inducing high strains and substantial grain refinement into material. In KoBo technique material

is extruded through a die that is in constant reversible rotation motion. This motion destabilizes structure by causing constant changes of deformation path. Destabilization stops formation of new dislocations which reduces deformation related strengthening, material is deformed by heterogeneous visco-plastic flow, extrusion force is reduced and high degree of processing in single pass is possible[6,7,8].

Polycrystalline zinc when subjected to SPD process exhibits improved mechanical strength $R_{0,2} \approx 160\text{MPa}$ and $R_m \approx 170\text{MPa}$ compared to the same material treated with conventional plastic deformation method ($R_{0,2} \approx 40\text{MPa}$,

* INSTITUTE OF METALLURGY AND MATERIALS SCIENCE POLISH ACADEMY OF SCIENCES, 30-059 KRAKÓW, 25 REYMONTA STR., POLAND

$R_m \approx 110$ MPa in material deformed conventionally until fracture). This increase in mechanical parameters is explained by Hall – Petch relation. While after conventional process mean diameter size of material is around $40 \mu\text{m}$, structure of zinc after SPD process consists of nano-scale grains [9].

However, Hall – Petch relation fails when applied to high purity (99.995%) polycrystalline zinc extruded by KoBo method. Mean grain diameter of extruded material was in range of couple of micrometers ($\sim 8 \mu\text{m}$) while achieved mechanical strength: $R_{0.2} \approx 150$ MPa and $R_m \approx 250$ MPa.

In presented work detailed microstructure and microstrain mapping investigation was carried out, in order to attempt an explanation of those properties.

2. Experimental procedure

High purity (99.995%) polycrystalline zinc ingot, 40 mm diameter was KoBo extruded at room temperature. Extrusion die diameter was 2 mm (extrusion ratio of $\lambda = 400$) and it was oscillating during extrusion process by an angle $\pm 8^\circ$ at frequency of 5 Hz. Speed of extrusion (ingot) was 0.5 mm/s. Samples for EBSD investigations have been prepared from both initial and KoBo extruded material. Preparation method for all samples consisted of mechanical grinding and polishing (SiC papers and diamond polishing suspensions and pastes) followed with electropolishing step. Precautions have been taken in order to avoid preparation induced deformation in surface layers of the material. Orientation Microscopy was performed by means of Electron BackScattered Diffraction method (EBSD) in FEI Quanta 3D FEG scanning electron microscope (SEM).

2.1. EBSD/SEM strain mapping

In EBSD method crystal orientation determination is based upon recognition of pairs of diffraction lines in Electron Backscattered Pattern (EBSP) and depends exclusively on geometry of K-lines related to specific crystallographic planes satisfying the Bragg condition, and not on their intensity [10]. Therefore EBSP's can be used for high precision determination of crystallographic orientation in large number of points in scanned areas, given that crystal lattice in those points is relatively undistorted or in other words has low concentration of lattice defects. EBSP's are highly sensitive to every kind of crystal lattice imperfections such as inherent or preparation introduced defects, strain fields, surface topography, impurities and so on. High concentrations of such defects can substantially distort or degrade diffraction patterns. In those cases indexing of diffraction pattern might not be possible and proper orientation determination cannot be performed. However even in cases of unindexable diffraction patterns it is almost always possible to determine their image quality parameters for instance Image Quality factor. Such factors can be calculated and recorded for each point in scanned area, and though they are dependent on many parameters such as state of sample lattice deformation, surface topography, atomic number and also apparatus factors, they can provide valuable qualitative information in certain scenarios.

As said before quality of EBSP is strongly affected by local concentration of lattice defects. Each defect of a crystal

lattice is related to local lattice strain in near vicinity of such defect. If electrons were to be diffracted on crystallite where such strains (third order strains) are present, K-lines in diffraction pattern would be diffusively broadened [11] and extent of this broadening effect would be related to concentration of defects and length of Burgers vector of those defects.

On the other hand second and first order strain fields are associated with homogeneous elastic deformation of grains, that in atomic scale is realized by change of distance between atomic layers in direction of induced or inherent strains. Observed in EBSP's effect of such change in atomic layers spacing, is change in position of K-lines (shift) in relation to unstrained material [12]. Pairs of K-lines can be either closer or further apart from each other depending on nature of strain (tensile or compressive).

Effects from both types of lattice distortion are affecting diffraction pattern recorded for specific points in scanned area. By defining and determining IQ factors for all scanned points in EBSD measurement one could assess spatial distribution of local crystal lattice strains originated from different kinds of effects. IQ factor maps are effective way to observe grain boundaries, lattice deformation fields and gradients and dislocations stacks or networks.

In presented investigation IQ maps were used to determine distribution of crystal lattice defect related distortions, fraction of distorted lattice, topography and distribution of defects in vicinity of grain boundaries and dislocation structures of the insides of grains.

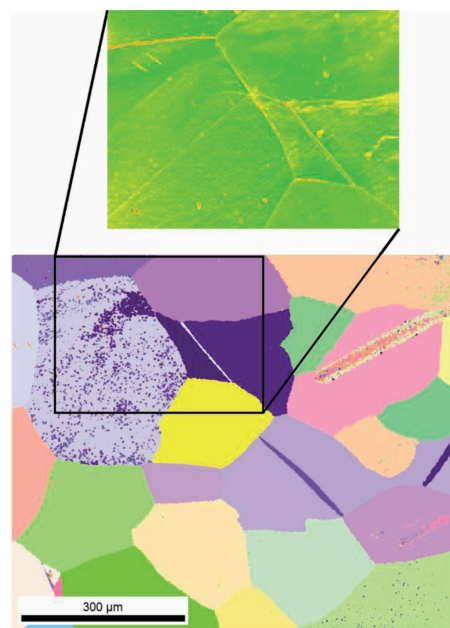


Fig. 1. Microstructure (IPF map) of initial state of zinc based on EBSD measurement. Expanded area map shows distribution of IQ factor: green – high IQ value, yellow – low IQ value

3. Results

3.1. Microstructure, crystal orientation analysis

Initial state zinc consists of large recrystallized, equiaxed grains of diameter in range of hundreds of micrometers (from

around one to five hundreds of microns) as shown on Inverted Pole Figure (IPF) map: Fig. 1.

Microstructure of KoBo extruded zinc was found to be highly heterogeneous and consisting of both fine and large primary grains. Grains sizes evaluated on the basis of EBSD analysis are ranging from sub micron to over one hundred microns. The highest level of grain refinement is observed in surface layers of extruded wire. Microstructure in areas closer to center of sample features much larger, primary grains at different stages of fragmentation. Grains are slightly elongated in the direction of extrusion, which is visible on longitudinal section of KoBo extruded sample Fig. 2b.

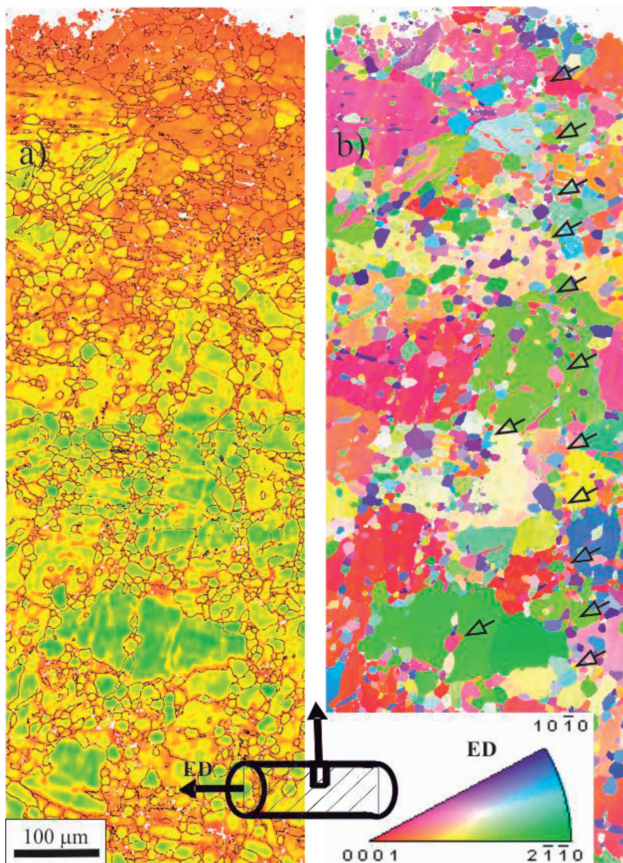


Fig. 2. Longitudinal section of KoBo extruded zinc wire, scan taken along radius of the wire. a) IQ factor map from values color coded: green – high IQ, yellow – medium, red – low IQ; HAGBs indicated with black line; b) IPF map, intergranular bands indicated with arrows

Microstructure of longitudinal section reveals characteristic intergranular bands of fine equiaxed grains indicated with arrows on Fig. 2b. Those bands extend through the entire thickness of wire while intersecting multiple coarse grains and are oriented at angles ranging from 60 to 90 degrees to the extrusion direction.

High angle grain boundaries (HAGBs) are well developed, and their thickness estimated from the rate of crystallographic orientation change does not exceed a few hundred nanometers and is similar to that in the input material Fig. 3.

Careful analysis of subtle orientation changes of crystal lattice within the grains and near grain boundaries in most cases indicates statistically stored dislocations (SSDs) [12] and accumulations of point lattice defects Fig. 4. Some individual

grains exhibits distinct curvature of the lattice which has to be realized by geometrically necessary dislocations (GNDs) [13,14] like shown on Fig. 5.

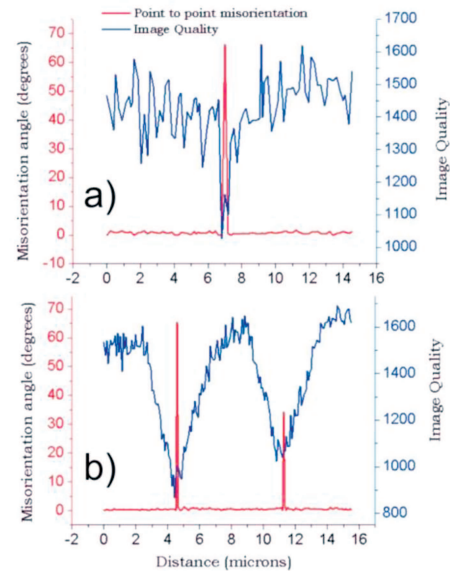


Fig. 3. Cross section through HAGB showing variation of IQ factor (blue line) and point to point misorientation angle (red line) in: a) initial sample; b) KoBo extruded sample

Analysis of orientations fluctuations in some large primary grains (Fig. 6.) reveals tendency to form dislocations walls within those grains, and fragmentation into similarly oriented blocks.

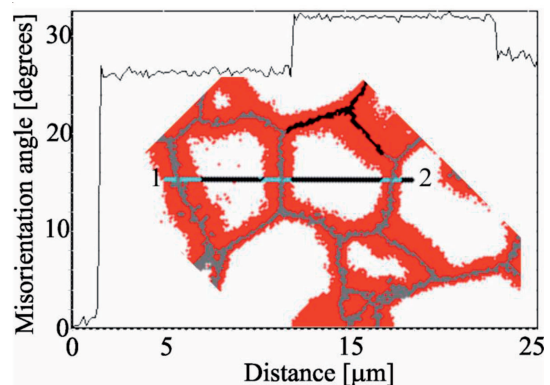


Fig. 4. Microstructure of zinc after KoBo extrusion. Regions with highly deformed crystal lattice (low values of IQ factor) are indicated with red colour. Insides of grains with low density of defects are presented by white areas. HAGBs marked with black lines. Point to origin misorientation angles along cross section (points 1 to 2) through two typical grains are presented on graph

These results obtained from analysis of misorientation changes measured in EBSD SEM technique, while useful, are indirect indication of defects in characterized microstructure. Therefore in order to determine exact nature of observed misorientation fluctuations (whether they are related to dislocations or other type of crystal defects) inside grains and at their boundaries, further investigations utilizing TEM and orientation microscopy in TEM are going to be carried out.

3.2. Strain mapping/IQ factors analysis

The most characteristic feature of microstructure revealed by analysis of IQ factor distribution are thick areas of highly distorted lattice (low IQ) adjacent to grain boundaries. While grain interiors are mainly characterized by high IQ and therefore relatively undistorted crystal lattice, areas stretched along grain boundaries contain high density of crystal defects, resulting in low values of IQ factor in those regions of microstructure (Fig. 4).

Thickness of grain boundary distortion areas was measured and found to be in order of several micrometers. This stands in direct contrast to situation observed in sample of initial (non deformed) zinc, where such distorted areas are also present, however their thickness relates closely to thickness of grain boundary (determined from misorientation change rate) and on average is in order of one micron (Fig. 1.) In case of KoBo deformed material grain boundary distortion areas are much broader than what it is expected from thickness of grain boundaries themselves.

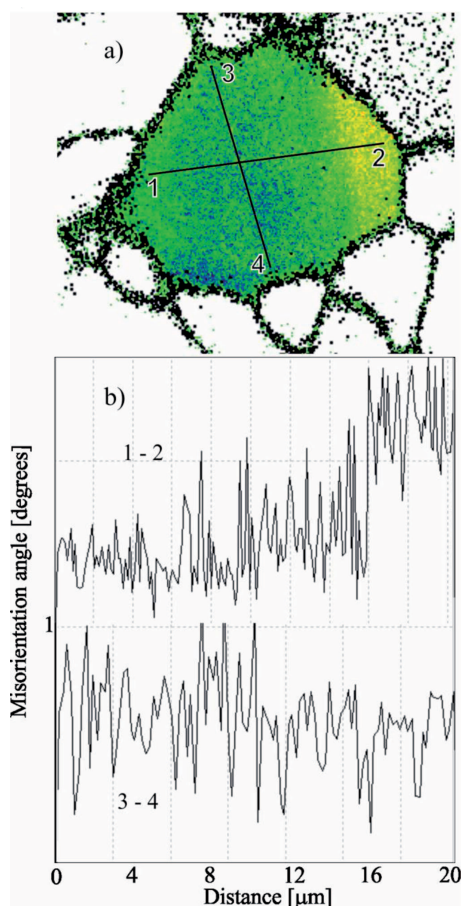


Fig. 5. a) Subtle misorientation change analysis in grain with crystal lattice bending. b) Point to origin misorientation variation profile (points 1-2) indicates curvature of lattice realized by geometrically necessary dislocations (GNDs)

Thick areas of distorted lattice associated with grain boundaries, are accounting for relatively high fraction of microstructure, which is directly related to grain refinement and grain boundary content. The highest fraction of distorted crystal lattice, up to 60% is observed in the external layers of material, which is consistent with higher levels of grain re-

finement in those areas. Within the sample around 30% of lattice is characterized with high levels of distortion.

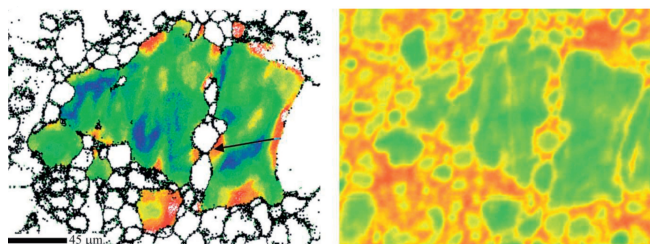


Fig. 6. Microstructure of KoBo extruded zinc: large, partially fragmented primary grain. Left: Orientation fluctuations inside grain. Misorientation angle in respect to selected basal orientation is colour coded: blue 0°, green ~2°, red ~4°. Arrow indicates fine recrystallized grains forming a band.

Right: Topography of crystal lattice defect concentration (indicated by IQ values): green – low concentration, yellow – medium, red – high concentration of defects

4. Conclusion

Microstructure of KoBo extruded polycrystalline zinc is highly heterogeneous and consists of grains with various refinement degree and elongated slightly in the direction of extruded wire axis.

Grains sizes are varying from under a micron to over one hundred microns. High angle grain boundaries are well developed and their thickness does not exceed few hundred nanometers, similarly to grain boundaries in initial material.

The highest level of grain refinement and the highest fraction of deformed lattice is observed in the topmost layers of the material. Analysis of subtle orientation changes inside grains and in areas close to grain boundaries suggest that in most cases plastic strain of lattice is associated with randomly stacked dislocations and/or point defects. Fraction of highly distorted crystal lattice is as high as 30% within the sample and even 60% in surface layers.

Analysis of spatial distribution of localized microstructure distortions, revealed composite like arrangement of features in the deformed material microstructure, which is the most distinctive characteristic of KoBo extruded zinc. Material was found to be consisting of grains with relatively undistorted crystallographic lattice, surrounded by thick areas of highly distorted lattice adjacent to grain boundaries. This structure of soft defect-free grains and harder, distorted "shell" is believed to be responsible for increased mechanical strength of KoBo extruded zinc. Exact crystallographic nature of observed microstructure distortions is going to be further investigated by means of TEM and crystal orientation microscopy in TEM.

Acknowledgements

This work was co-financed by the European Union from resources of the European Social Fund (Project No.POKL.04.01.00-00-004/10) and supported by grant from Polish National Scientific Center (NCN):2011/03/B/ST8/06120.

REFERENCES

- [1] R.Z. Valiev, R.K. Islamgaliev, I.V. Alexandrov, *Prog Mater Sci.* **45**, 103-189 (2000).
- [2] Y.T. Zhu, T.G. Langdon, *JOM.* 58-63 October 2004.
- [3] M.A. Meyers, A. Mishra, D.J. Benson, *Prog Mater Sci.* **51**, 427-556 (2006).
- [4] K.S. Kumar, H. Van Swygenhoven, S. Suresh, *Acta Mater* **51**, 5743-5774 (2003).
- [5] A. Korbel, W. Bochniak, European Patent No. 0711210, U.S. Patent No. 573959.
- [6] A. Korbel, W. Bochniak, P. Ostachowski, L. Blaz, *Metall Mater Trans A.* **42A**, 2881-2897 (2011).
- [7] A. Korbel, W. Bochniak, *SCRIPTA MATER.* **51**, 755-759 (2004).
- [8] A. Korbel, J. Pospiech, W. Bochniak, A. Tarasek, P. Ostachowski, J. Bonarski, *Int J Mat Res.* **102**, 464-473 (2011).
- [9] X. Zhang, H. Wang, R.O. Scattergood, J. Narayan, C.C. Koch, A.V. Sergueeva, A.K. Mukherjee, *Acta Mater.* **50**, 4823-4830 (2002).
- [10] R.A. Schwarzer, D.P. Field, B.L. Adams, M. Kumar, A.J. Schwartz, Present State of Electron Backscatter Diffraction and Prospective Developments in A.J. Schwartz, M. Kumar, B.L. Adams, D.P. Field (Ed) *Electron Backscatter Diffraction in Materials Science*, Second Edition, Springer 2009.
- [11] K. Sztwiertnia, *Orientacja krystalograficzna w badaniach mikrostruktury materiałów*, Kraków 2009.
- [12] S.I. Wright, M.M. Nowell, D.P. Field, *Microsc Microanal.* **17**, 316-329 (2011).
- [13] L.N. Brewer, D.P. Field, C.C. Merriman, Mapping and Assessing Plastic Deformation Using EBSD in A.J. Schwartz, M. Kumar, B.L. Adams, D.P. Field (Ed) *Electron Backscatter Diffraction in Materials Science*, Second Edition, Springer 2009.
- [14] H. Gao, Y. Huang, *Scripta Mater.* **48**, 113-118 (2003).